

Attractions between Like-Charged Surfaces with Dumbbell-Shaped Counterions

Yong Woon Kim,^{1,2} Juyeon Yi,³ and P. A. Pincus^{2,4}

¹*School of Physics, Korea Institute for Advanced Study, Seoul 130-722, Korea*

²*Materials Research Laboratory, University of California, Santa Barbara, California 93106, USA*

³*Department of Physics, Pusan National University, Busan 609-735, Korea*

⁴*Department of Physics, Korea Advanced Institute of Science and Technology, Daejeon 305-701, Korea*
(Received 27 November 2007; revised manuscript received 8 July 2008; published 14 November 2008)

We study the effect of dumbbell-like counterions on the interactions between similarly charged surfaces. Via a systematic study using Monte Carlo simulations and field theory, we fully consider electrostatic correlations and ion structure and find that their intricate coupling determines the equilibrium phase behaviors. In particular, an energetic bridging mechanism is revealed to cause surface attractions for a finite range of surface separations, even in the Poisson-Boltzmann limit.

DOI: 10.1103/PhysRevLett.101.208305

PACS numbers: 82.70.-y, 61.20.Ja, 82.70.Dd, 87.15.-v

The role of ions in solution mediating interactions between charged objects is a subject of fundamental importance in a multitude of industrial processes and biological systems. A classical approach based on the mean field Poisson-Boltzmann (PB) theory has been used to explain many interesting features. Yet, due to the complexity of systems with Coulomb interactions, a complete understanding is still lacking. For instance, like-charge attractions in the presence of multivalent counterions [1] cannot be interpreted by the PB theory. There have been several attempts toward achieving a better understanding by including factors discarded in PB theory, e.g., steric effects [2], nonuniform dipolar features of solvent molecules [3], and the counterion correlations [4,5].

For certain multivalent ions, the separations between charges in an ion are too large to be ignored, leading to breakdown of the pointlike picture of ions assumed in the PB theory [6]. Furthermore, the internal structure of a dumbbell-like counterions has been shown to have considerable influence on virus condensation [7] and phase equilibria of electrolytes [8]. It is also known that DNA condensation is effectively driven by short stiff polyamines such as spermine and spermidine which can be viewed as rodlike ions [9]. In this respect, ion structure is anticipated to play a crucial role in the interactions between charged bodies. In this Letter, we address this problem and present a systematic study on a system consisting of two likely charged plates and dumbbell-like counterions as a minimal model for ions with an internal structure. In fact, by adopting a similar model for divalent rodlike ions, Bohinc *et al.* obtained a PB equation valid in the limit of small rod size [10]. The electrostatic correlations for an arbitrary dumbbell size still need to be considered for a comprehensive picture. To this end, we perform extensive Monte Carlo (MC) simulations for a wide range of parameter space. In parallel, we formulate a field theory that extends the PB and strong-coupling (SC) theories for point charges [5] to the case of dumbbell-like counterions. We find that the rods oriented perpendicular to the surface,

forming a bridging configuration across the midplane, energetically pull the surfaces even in the PB regime. At intermediate coupling strengths, the bridging effect continues to exist and interplays with electrostatic correlation. In the strong-coupling limit, it becomes insignificant, and in turn electrostatic correlations prevail.

Consider N dumbbell-shaped counterions distributed between two like-charged surfaces with surface charge density σ and intersurface distance D . We model a single dumbbell ion by two q -valent point charges separated by a fixed distance d , and introduce the ion number density operator $\rho(\mathbf{r}) = \sum_{j=1}^N [\delta(\mathbf{r} - \mathbf{r}_j) + \delta(\mathbf{r} - \mathbf{r}_j - \mathbf{d}_j)]$ with $\mathbf{d}_j = d\hat{\Omega}_j$ where $\hat{\Omega}_j$ is a unit vector indicating the dumbbell orientation. The electrostatic Hamiltonian of the system is

$$\mathcal{H}_e = \mathcal{H}/k_B T = \frac{\ell_B}{2} \int d\mathbf{r} d\mathbf{r}' Q(\mathbf{r}) v(\mathbf{r}, \mathbf{r}') Q(\mathbf{r}') \quad (1)$$

with the Coulomb interaction kernel, $v(\mathbf{r}, \mathbf{r}') = 1/|\mathbf{r} - \mathbf{r}'|$, and the Bjerrum length $\ell_B \equiv e^2/\epsilon k_B T$. The charge density at position \mathbf{r} is given by $Q(\mathbf{r}) = q\rho(\mathbf{r}) - \sigma(\mathbf{r})$ with $\sigma(\mathbf{r}) = \sigma[\delta(z) + \delta(z - D)]$. We consider the partition function in the grand canonical ensemble, $\mathcal{Q}_\lambda = \sum_{N=0}^{\infty} \lambda^N Z_N$ with fugacity λ and the canonical partition function Z_N ,

$$Z_N = \prod_{j=1}^N \int_C \frac{d\mathbf{r}_j d\Omega_j}{N! 4\pi} \exp\left[-(\mathcal{H}_e - \Sigma_s) + \int d\mathbf{r} h(\mathbf{r}) \rho(\mathbf{r})\right]. \quad (2)$$

The integral should be done under the geometrical constraint C , i.e., $z \in (0, D)$. The second term Σ_s in the exponent is for subtracting all the self-energy terms containing $v(\mathbf{r}, \mathbf{r})$. The auxiliary field $h(\mathbf{r})$ is introduced to evaluate the mean number density. After a Hubbard-Stratonovitch transformation followed by the Gaussian integral over $\rho(\mathbf{r})$, we are left with the partition $\mathcal{Q}_\lambda = Z_v \int \mathcal{D}\phi e^{-G[\phi]}$ with $Z_v^{-1} = \det[v(\mathbf{r}, \mathbf{r}')]^{1/2}$. The effective action is given by

$$G = \frac{1}{8\pi\Xi} \int_C d\tilde{\mathbf{r}} \left\{ (\tilde{\nabla}\phi)^2 - 4\Lambda \int d\tilde{\Omega} e^{-\phi_h(\tilde{\mathbf{r}}) - \phi_h(\tilde{\mathbf{r}}+\tilde{\mathbf{d}})} \right\} - G_b \quad (3)$$

where Ξ is the coupling parameter, $\Xi = 2\pi q^3 \ell_B^2 \sigma$, rescaled fugacity $\Lambda = \lambda/2\pi\sigma^2 \ell_B$, and $\phi_h(\mathbf{r}) = i\phi(\mathbf{r}) - h(\mathbf{r})$. Here, the solid angle $\tilde{\Omega}$ and $\tilde{\mathbf{r}}$ are rescaled variables, respectively, as $\tilde{\Omega} = \Omega/4\pi$ and $\tilde{\mathbf{r}} = \mathbf{r}/\mu$ with the Gouy-Chapmann length, $\mu = 1/2\pi\ell_B q\sigma$. For simplicity of notation, hereafter we shall drop the tilde on the scaled length. The boundary contribution from the surface charge reads $G_b = -(i/2\pi\Xi) \int d\mathbf{r} \sigma(\mathbf{r}) \phi(\mathbf{r})$.

We evaluate the expectation value of the ion number density given by $\langle \rho(\mathbf{r}) \rangle = \delta \ln \mathcal{Q}_\Lambda / \delta h(\mathbf{r}) \mu^3 |_{h(\mathbf{r})=0}$, or

$$\tilde{\rho}(\mathbf{r}) = \frac{\rho(\mathbf{r})}{2\pi\ell_B\sigma^2} = 2\Lambda \left\langle \int_C d\Omega e^{-i\phi(\mathbf{r}) - i\phi(\mathbf{r}+\mathbf{d})} \right\rangle, \quad (4)$$

where $\langle X \rangle = \int \mathcal{D}\phi X e^{-G} / \mathcal{Q}_\Lambda$. An approximate evaluation of \mathcal{Q}_Λ can be done either for $\Xi \ll 1$ or for $\Xi \gg 1$. Considering first the former case via the saddle point approximation, we have $\ln \mathcal{Q}_\Lambda \approx -G[\phi_{\text{PB}}]$ with ϕ_{PB} ensuring $\delta G / \delta \phi(\mathbf{r}) |_{\phi=\phi_{\text{PB}}} = 0$, which leads to the extended PB equation for dumbbell ions as

$$\frac{\partial^2}{\partial z^2} i\phi_{\text{PB}}(z) = -4\Lambda \int_C d\Omega e^{-i\phi_{\text{PB}}(z) - i\phi_{\text{PB}}(z+d_z)}. \quad (5)$$

Accordingly, from Eq. (4), the PB density profile reads as

$$\tilde{\rho}_{\text{PB}}(z) = -2\Lambda \int_C d\Omega e^{-i\phi_{\text{PB}}(z) - i\phi_{\text{PB}}(z+d_z)}, \quad (6)$$

where the fugacity Λ should be determined by requiring the charge neutrality of the system, $\int dz \tilde{\rho}_{\text{PB}}(z) = 2$.

In the opposite strong-coupling limit, $\Xi \gg 1$, the virial expansion of the partition function as a power series in Λ/Ξ is efficient. Retaining terms up to linear order in the expansion parameter, we write

$$\frac{\mathcal{Q}_\Lambda}{\mathcal{Q}_{\Lambda=0}} \approx 1 + \frac{\Lambda}{2\pi\Xi} \left\langle \sum_j \int_C d\mathbf{r} d\Omega e^{-\phi_h(\mathbf{r}) - \phi_h(\mathbf{r}+\mathbf{d})} \right\rangle_{\Lambda=0} \quad (7)$$

which is further simplified by shifting the field as $\tilde{\phi}(\mathbf{r}) = \phi(\mathbf{r}) + i\Xi \int d\mathbf{r}' v(\mathbf{r}, \mathbf{r}') [\delta(\mathbf{r}' - \mathbf{r}) + \delta(\mathbf{r}' - \mathbf{r} - \mathbf{d})]$. It is then straightforward to see that SC density profile is given by

$$\tilde{\rho}_{\text{SC}}(z) = 2\Lambda \int_C d\Omega e^{-\Xi/d}, \quad (8)$$

where the fugacity Λ is again determined by imposing the charge neutrality. Counting the rotational restriction, for example, when $d < D < 2d$, the SC density reduces to

$$\tilde{\rho}_{\text{SC}}(z) = 2\Omega(z, d)/(D - d/2). \quad (9)$$

Here, the solid angle function, $\Omega(z, d) = \int_C d\Omega/4\pi$, describes the accessible volume fraction associated with rod rotation: $\Omega(z, d) = (1 + z/d)/2$ for $z \in (0, D - d)$ and $D/2d$ for $z \in (D - d, d)$. On the other hand, when $D < d$,

$$\tilde{\rho}_{\text{SC}}(z) = 4\Omega(z, d)(d/D^2) = 2/D, \quad (10)$$

since $\Omega(z, d) = D/2d$ for $z \in (0, D)$.

In order to fill the gap between PB and SC theory, MC simulations are conducted in the canonical ensemble. Periodic boundary conditions are imposed on the lateral directions in order to minimize the finite system size effects. In Fig. 1, we show the ion density distribution $\tilde{\rho}(z)$ of small dumbbell ions ($d = 0.5$) in the limit of (a) PB and (b) SC regimes for different surface separations. For both regimes, the MC results (symbols) show an excellent agreement with the theoretical predictions (solid lines) obtained from Eqs. (6) and (8) [11]. It is notable that the surface density is significantly reduced in comparison with that of pointlike ions [for which PB solutions are plotted as dotted lines in Fig. 1(a)]. This demonstrates a natural tendency to lower the entropic cost of rotational restriction close to the surface.

Using the relation $P = \partial \ln Z_N / A \partial D$, we have confirmed that the contact value theorem is in general valid for dumbbell-like ions: the interplate pressure P is given by $\tilde{P} = P/2\pi\ell_B\sigma^2 = \tilde{\rho}(0) - 1$. Figure 2(a) displays the pressures for small dumbbell ions (open symbols) in comparison with those for pointlike ions (filled symbols) at various coupling parameters. The lines represent the analytic predictions for PB (solid line) and SC (dashed line) regime, well corresponding with the MC results. In the PB

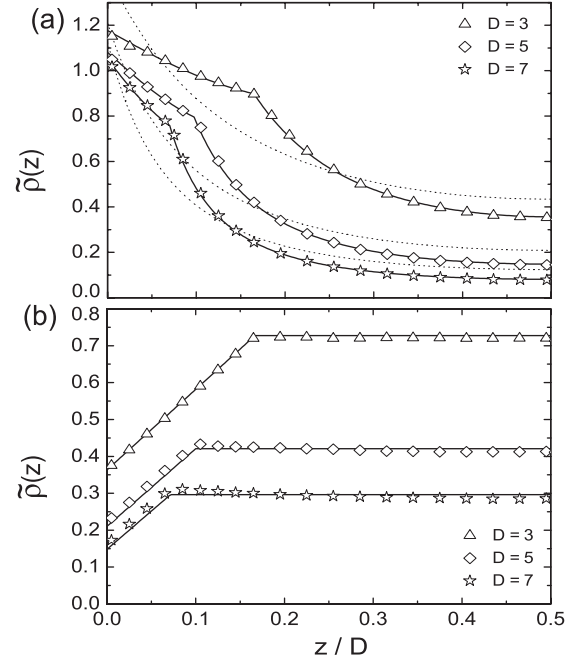


FIG. 1. Counterion density profiles $\tilde{\rho}(z)$ for small dumbbell ions with $d = 0.5$ in the (a) PB limit [$\Xi = 0.05$] and (b) SC limit [$\Xi = 10^4$]. The data points are MC results for various surface separations. In (a), solid lines and dotted lines represent PB predictions for dumbbell-like ions [Eq. (6)] and for pointlike ions, respectively, whereas solid lines in (b) are SC predictions [Eq. (8)].

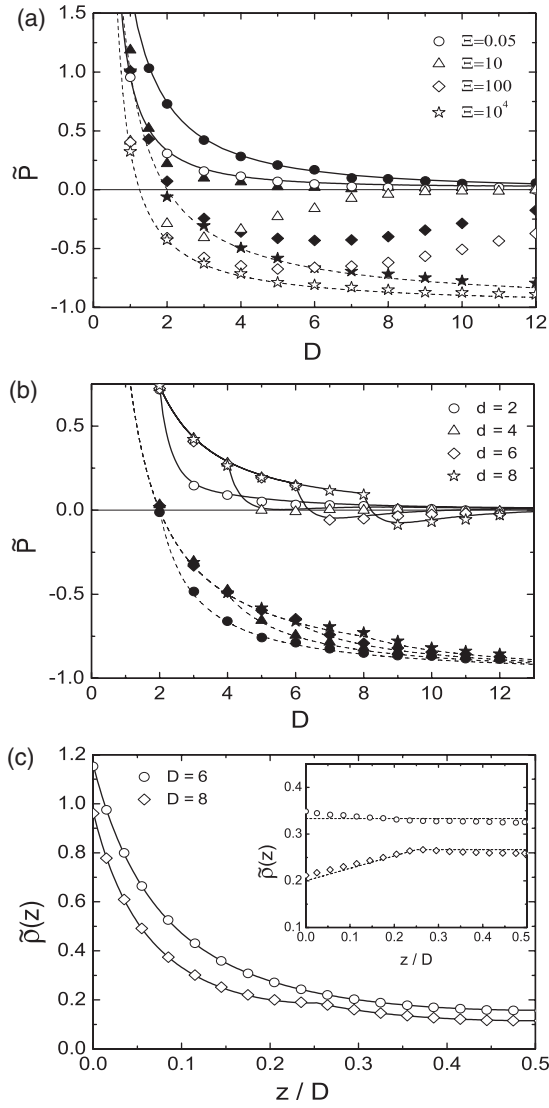


FIG. 2. Pressure as a function of the plate separation D (a) for small dumbbell ions of $d = 0.5$ with various values of Ξ and (b) for large dumbbell ions at $\Xi = 0.05$ (open symbols) and at $\Xi = 10^4$ (filled symbols). In (a) and (b), solid and dashed lines denote PB [Eq. (6)] and SC [Eq. (8)] predictions for respective dumbbell sizes. For comparison, pressures for the equivalent system consisting of pointlike ions and having the same surface charge are plotted together in (a): MC simulations (filled symbols), PB (solid), and SC (dashed) solutions. (c) density profiles for large dumbbells of $d = 6$ at $\Xi = 0.05$ with $\tilde{\rho}_{PB}$ [Eq. (6): line]. Inset shows the same at $\Xi = 10^4$ with $\tilde{\rho}_{SC}$ [Eq. (8): line].

and SC limit, it is reasonable for vanishing d/D to expect no significant difference between dumbbell-like and pointlike pictures except that μ for rod ions is reduced as half since $q \rightarrow 2q$. What then happens as d increases to a large value? Figures 2(b) and 2(c) present the pressure and ion density profile, respectively, for large dumbbell ions, where the theoretical predictions again well agree with the MC results. Surprisingly, Fig. 2(b) shows that as d increases, dumbbell counterions begin to mediate an attraction even at the PB level ($\Xi = 0.05$). This surface

attraction, arising from dumbbell structure combined with the electrostatic nature of the system, can be understood by the energetic consideration as follows.

Suppose a test dumbbell lying across the midplane under a symmetric electrostatic potential with negative curvature. When $d < D < 2d$, two charges of a dumbbell cannot reach both potential minima simultaneously. In this case, one can easily see that the energy minimum is achieved by the so-called bridging configuration where one end touches a wall ($z_1 = 0$) and the other is perpendicularly oriented towards the opposite surface ($z_2 = d > D/2$). The energy difference between these bridging configurations for varying D is given by $\Delta E = E(D + \delta D) - E(D)$ with $E(D) = i\phi(z_1; D) + i\phi(z_2; D)$. It can be readily found that $\partial E/\partial D = -i\phi'(0)(\partial\Lambda^{1/2}/\partial D)D > 0$ since $i\phi'(0) = 2$ and $\partial\Lambda^{1/2}/\partial D < 0$, clearly indicating the energetic driving to smaller D . On the other hand, when $D < d$, two charges in a dumbbell are free to reach both potential minima independently of each other, and the dumbbell ions behave exactly like $2N$ point charges, giving normal repulsive PB behaviors [12]. When $D > 2d$, the rods cannot form the bridging configuration; the surface touching rod cannot cross the midplane, yielding the energetic repulsion again. It is therefore conceivable that the attraction can occur only for $d < D < 2d$ if the bridging configurations prevail. In order to have an attraction, the total energy gain, $E(2d) - E(d)$ (which is shown to increase with d), should dominate over the entropic contributions of the order of $k_B T$, implying the existence of critical dumbbell size d^* for attractions. Note this picture of the energetic bridging does not hold for the SC regime where the electrostatic potential appears to be flat. It is also important to appreciate that the energetic bridging mechanism [13] is fundamentally different from the conventional entropic bridging attraction observed for polyelectrolyte-macroions complexes [14] where a chain connecting two surfaces experiences an entropic-elastic force.

Finally, we obtain the phase diagram of intersurface interactions as a function of D and d for various Ξ . Phase boundary data in Fig. 3 is determined from MC simulations by the value of D at which interplate pressure changes its sign. Regions bounded by curves thus represent negative interplate pressure at corresponding Ξ , explicitly showing the existence of attraction for all coupling strengths. Theoretic predictions denoted by dashed (SC) and dotted (PB) lines quantitatively agree with MC results. For small Ξ , a finite dumbbell size ($d > d^* = 4.2$) is required to form bound states. As consistent with the aforementioned picture, the attraction indeed occurs in the region of $d < D < 2d$ for large d , leading to the equilibrium plate separation (lower branch of curves) $D^* = d$. In the limit of large Ξ , according to Eqs. (9) and (10), $D^* = d/2 + 1$ for $D^* > d$ and $D^* = 2$ for $D^* < d$, suggesting different roles of structural characteristics of rod. When $D < d$, a dumbbell ion is viewed as structureless point charges and the electrostatic correlation dominates,

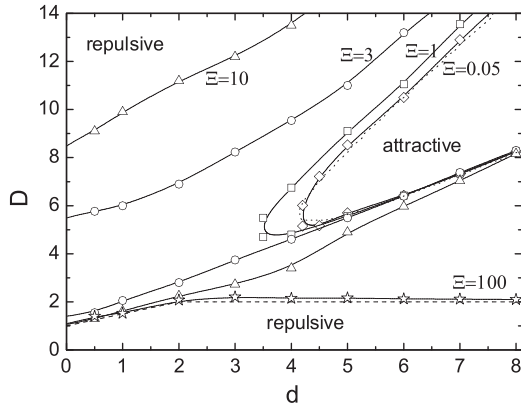


FIG. 3. Phase diagram obtained from MC simulations as a function of dumbbell size d and interplate separation D for various Ξ : Regions bounded by the curves indicate the negative interplate pressure at corresponding Ξ . Dotted line denotes the PB prediction from Eq. (6), whereas dashed line is the SC prediction from Eq. (8).

whereas for $D > d$, the depletion due to the rotational entropic reduction [$\Omega(z, d)$ in Eq. (9)] comes into play along, giving the d -dependent D^* .

Despite many studies devoted to polyelectrolyte-macroion complexes [14], only recently have there been theoretical studies to address the influence of chain stiffness of charged polymers on surface interactions with polyelectrolytes [15]. To some extent, short stiff polyelectrolytes bear a resemblance to multivalent dumbbell-like ions. According to Turesson *et al.* [15], the equilibrium surface separation is barely affected by the length of rigid stiff chains, consistent with our finding for large Ξ and d [16]. However, this is not the whole story, but the important factor determining phase behavior is the delicate competition among the entropic depletion, the electrostatic correlation, and the energetic bridging. Our study shows that in the weak coupling regime, the sufficient energy gain associated with bridging configurations is required to have an attraction, leading to $D^* \sim d$ only for $d > d^*$. In the strong-coupling regime, electrostatic correlation dominates, and for small $d < D^*$, depletion effect also plays a role. In the intermediate regime which is probably the most important for practical applications, the energetic bridging always collaborates with the electrostatic correlation, giving rise to the attractions for an arbitrary d and $D^* \sim d$. Predictions made in this study can be probed by means of x-ray scattering or surface force apparatus experiments. Extension of the present study to a system consisting of charged multicylinders with dumbbell ions would be interesting and will enable us to directly compare with experiments on M14 virus [7].

On completing this work, we learned that May *et al.* [17] considered a similar problem, symmetric electrolyte containing rodlike ions, as an extension of [10]: They presented a variational theory in the PB limit where interionic correlations are neglected, while our work is based on a

formal field theory, accompanied by systematic MC simulations, to cover all coupling strengths.

We would like to thank D. Andelman for helpful discussions. The authors acknowledge support from NSF under Grants Nos. DMR 05-03347 and DMR 07-10521. J. Y. also acknowledges support from the Korea Research Foundation Grant funded by the Korean Government (MOEHRD) (Grant No. KRF-2006-005-J02804).

- [1] V. A. Bloomfield, *Biopolymers* **31**, 1471 (1991); V. A. Bloomfield, *Curr. Opin. Struct. Biol.* **6**, 334 (1996); J. X. Tang, S. Wong, P. Tran, and P. Janmey, *Ber. Bunsen-Ges. Phys. Chem.* **100**, 796 (1996); N. Grønbech-Jensen, R. J. Mashl, R. F. Bruinsma, and W. M. Gelbart, *Phys. Rev. Lett.* **78**, 2477 (1997); R. Podgornik, D. Rau, and V. A. Parsegian, *Biophys. J.* **66**, 962 (1994).
- [2] I. Borukhov, D. Andelman, and H. Orland, *Phys. Rev. Lett.* **79**, 435 (1997); Y. Burak and D. Andelman, *J. Chem. Phys.* **114**, 3271 (2001).
- [3] A. Abrashkin, D. Andelman, and H. Orland, *Phys. Rev. Lett.* **99**, 077801 (2007).
- [4] Y. Levin, *Rep. Prog. Phys.* **65**, 1577 (2002) and references therein.
- [5] A. G. Moreira and R. R. Netz, *Phys. Rev. Lett.* **87**, 078301 (2001).
- [6] O. Alvarez, M. Brodwick, R. Latorre, A. McLaughlin, S. McLaughlin, and G. Szabo, *Biophys. J.* **44**, 333 (1983).
- [7] J. C. Butler, T. Angelini, J. X. Tang, and G. C. L. Wong, *Phys. Rev. Lett.* **91**, 028301 (2003).
- [8] Q. Yan and J. J. de Pablo, *Phys. Rev. Lett.* **88**, 095504 (2002).
- [9] J. Pelta, F. Livolant, and J.-L. Sikorav, *J. Biol. Chem.* **271**, 5656 (1996); E. Raspaud, M. O. de la Cruz, J.-L. Sikorav, and F. Livolant, *Biophys. J.* **74**, 381 (1998).
- [10] K. Bohinc, A. Iglic, and S. May, *Europhys. Lett.* **68**, 494 (2004).
- [11] Replacing integral with summation on a grid of points, we numerically solve Eq. (5) via relaxation method for two point boundary value problems.
- [12] For $D < d$, the pressure for N dumbbell ions with a finite size indeed exactly follows that for $2N$ point charges, implying a crossover at $D = d$ from N -particle system to $2N$ -particle system. This is responsible for the cusp of the pressure curve, or a discontinuity in compressibility, which is clearly shown in Fig. 2(b) but not in 2(a) due to the plot range of the ordinate.
- [13] H. Boroudjerdi and R. R. Netz, *Europhys. Lett.* **64**, 413 (2003); *J. Phys. Condens. Matter* **17**, S1137 (2005).
- [14] T. Åkesson, C. Woodward, and B. Jönsson, *J. Chem. Phys.* **91**, 2461 (1989); R. Podgornik, *J. Phys. Chem.* **95**, 5249 (1991); R. Podgornik, *J. Polym. Sci., Part B: Polym. Phys.* **42**, 3539 (2004) and references therein.
- [15] M. Turesson, J. Forsman, and T. Åkesson, *Langmuir* **22**, 5734 (2006).
- [16] They considered rigid chains made up of more than 10 monomers, each carrying an unit charge, which roughly corresponds to $q > 5$ and $\Xi > 385$ in our model.
- [17] S. May, A. Iglič, J. Rescic, S. Maset, and K. Bohinc, *J. Phys. Chem. B* **112**, 1685 (2008).